Presumptive TRP channel CED-11 promotes cell volume decrease and facilitates degradation of apoptotic cells in *Caenorhabditis elegans*

Kaitlin Driscoll[a], Gillian M. Stanfield[a,b], Rita Droste[a], and H. Robert Horvitz[a,1]

[a]Howard Hughes Medical Institute, Department of Biology, Massachusetts Institute of Technology, Cambridge, MA 02139; and [b]Department of Human Genetics, University of Utah, Salt Lake City, UT 84112

Contributed by H. Robert Horvitz, June 29, 2017 (sent for review March 28, 2017; reviewed by Barbara Conradt and Zheng Zhou)

Apoptotic cells undergo a series of morphological changes. These changes are dependent on caspase cleavage of downstream targets, but which targets are significant and how they facilitate the death process are not well understood. In *Caenorhabditis elegans* an increase in the refractility of the dying cell is a hallmark morphological change that is caspase dependent. We identify a presumptive transient receptor potential (TRP) cation channel, CED-11, that acts in the dying cell to promote the increase in apoptotic cell refractility. CED-11 is required for multiple other morphological changes during apoptosis, including an increase in electron density as visualized by electron microscopy and a decrease in cell volume. In *ced-11* mutants, the degradation of apoptotic cells is delayed. Mutation of *ced-11* does not cause an increase in cell survival but can enhance cell survival in other cell-death mutants, indicating that *ced-11* facilitates the death process. In short, *ced-11* acts downstream of caspase activation to promote the shrinkage, death, and degradation of apoptotic cells.

TRP channel | apoptosis | *C. elegans* | cell volume | apoptotic volume decrease

Apoptosis, also referred to as "programmed cell death," is defined by a set of morphological and biochemical changes in the dying cell (1, 2). These changes both reflect the death of the cell and prepare the cell for engulfment and degradation by phagocytes. Ineffective execution of apoptosis can lead to incomplete cellular degradation or to the survival of unwanted cells, events associated with diseases such as autoimmune disorders and cancer (3, 4). Both the death process and morphological changes that occur during apoptosis are initiated by cysteine proteases known as "caspases" (5, 6). Although proteomic studies have identified hundreds of proteins cleaved by caspases during apoptosis, many questions remain about how these proteins function during apoptosis and their contributions to the death process.

Cell shrinkage is a characteristic morphological change during apoptosis and has been used to differentiate apoptosis from necrosis, but the molecular mechanism and significance of apoptotic cell shrinkage are unclear (7). It has been hypothesized that cell shrinkage during apoptosis, termed "apoptotic volume decrease" (AVD), could occur through a mechanism similar to that of the regulatory volume decrease (RVD) most cells undergo when returning to a baseline volume after hypoosmotic-induced cell swelling (8). During RVD, potassium and chloride channels are activated, resulting in an efflux of potassium and chloride from the cell, followed by an efflux of water driven by the osmotic gradient (9).

In *Caenorhabditis elegans*, an increase in cell refractility as observed by Nomarski differential interference contrast (DIC) microscopy is one of the defining apoptotic morphological changes (10). The increase in the refractility of apoptotic cells is dependent on the CED-3 caspase (11). Many mutants have been identified in which refractile apoptotic cells persist unengulfed (12). From a screen for mutants that alter the accumulation of refractile apoptotic cells of a *ced-5* engulfment mutant, we discovered a gene, *ced-11*, that is required for the refractile appearance of apoptotic cells. *ced-11* encodes a presumptive transient receptor potential (TRP) channel. TRP channels are nonselective cation channels that participate in diverse sensory processes and can be involved in regulating RVD (13, 14). Like most TRP channels, the CED-11 protein can localize to the plasma membrane. We found that CED-11 is required for cell shrinkage, suggesting that it, along with other TRP family members, might have a mechanistically conserved role in cell volume regulation. We conclude that CED-11 acts in the dying cell directly or indirectly downstream of CED-3 activation to promote AVD and that without this change in volume apoptotic cells take longer to degrade and have an increased chance of survival.

Results

***ced-11* Is Required for the Highly Refractile Morphology of Apoptotic Cells.** *C. elegans* apoptotic cells acquire a raised, highly refractile appearance when visualized by DIC microscopy (Fig. 1*A*) (10). We identified the gene *ced-11* (*cell death-11*) in a screen for suppressors of the accumulation of refractile apoptotic cells that occurs in *ced-5* mutants, which are defective in the engulfment of apoptotic cells (Fig. 1 *B–D*). *ced-11; ced-5* mutants lack refractile apoptotic cells and instead contain flat disk-like cells that are distinct from living cells and that we hypothesized were nonrefractile apoptotic cells. We confirmed that the flat disk-like cells observed in *ced-11* animals are cells that normally undergo apoptosis: null alleles of *ced-3* and *ced-4*, which prevent apoptotic cell deaths, prevented the appearance of the flat disk-like cells in *ced-11; ced-3* and *ced-4 ced-11*

Significance

Apoptosis is required for normal animal development and homeostasis. Apoptosis is driven by caspases, cysteine proteases that cleave downstream targets and cause cell death and degradation. A classic hallmark of apoptosis is cell shrinkage. We identify a presumptive transient receptor potential (TRP) family cation channel, CED-11, that acts during apoptosis in *Caenorhabditis elegans* downstream of CED-3 caspase activation to promote a decrease in cell volume and facilitate the death and degradation of apoptotic cells. TRP channels can stimulate cell shrinkage in response to osmotic stress. Our results suggest that the mechanism of cell shrinkage during apoptosis might be similar to the regulatory volume decrease (RVD) that cells undergo after the cell swelling induced by hypoosmotic stress.

Author contributions: K.D., G.M.S., and H.R.H. designed research; K.D., G.M.S., and R.D. performed research; K.D. and G.M.S. contributed new reagents/analytic tools; K.D., G.M.S., R.D., and H.R.H. analyzed data; and K.D., G.M.S., and H.R.H. wrote the paper.

Reviewers: B.C., Ludwig-Maximilians Universitaet; and Z.Z., Baylor College of Medicine.

The authors declare no conflict of interest.

Freely available online through the PNAS open access option.

[1]To whom correspondence should be addressed. Email: horvitz@mit.edu.

This article contains supporting information online at www.pnas.org/lookup/suppl/doi:10.1073/pnas.1705084114/-/DCSupplemental.

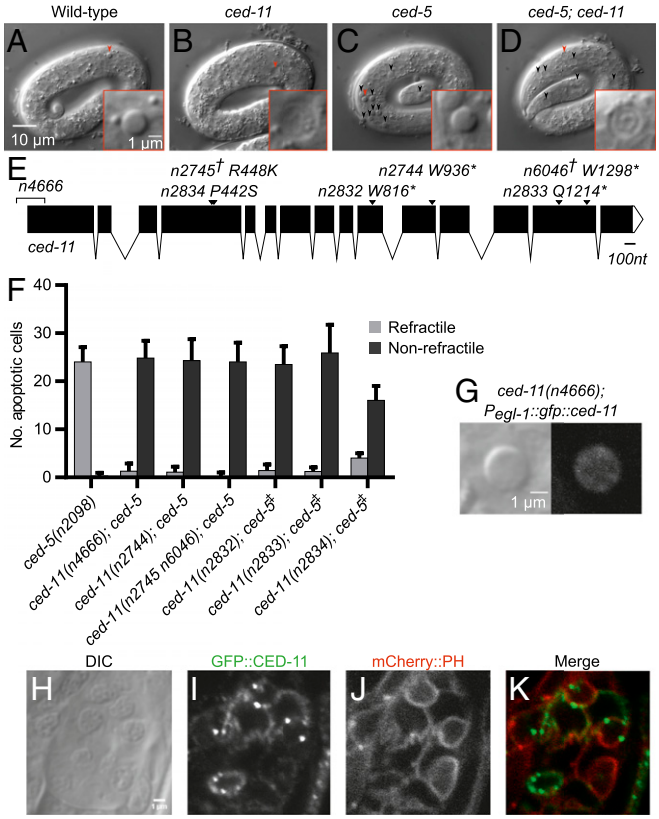

Fig. 1. *ced-11* is required for the increase in apoptotic cell refractility. (*A–D*) DIC images of threefold-stage embryos. Arrowheads indicate apoptotic cells that are shown in the *Insets*. (*A*) Wild-type embryo with refractile apoptotic cell. (*B*) *ced-11(n2744)* embryo with nonrefractile apoptotic cell. (*C*) *ced-5(n2098)* embryo with accumulated refractile apoptotic cells. (*D*) *ced-11(n2744); ced-5(n2098)* embryo with accumulated nonrefractile apoptotic cells. (*E*) Diagram of the *ced-11* gene. Arrows indicate the location of the *ced-11* allele. The asterisk indicates the stop codon. The dagger indicates two *ced-11* mutations isolated in the same strain. The bracket indicates a deletion. (*F*) Average numbers of refractile and nonrefractile apoptotic cells in the heads of threefold-stage embryos of the indicated genotypes. *ced-5(n2098)* was in all strains. The double-dagger indicates that the strain also includes *sem-4(n1378)*. Error bars indicate SD. ($n > 20$). (*G*) DIC and GFP images of a refractile apoptotic cell that expresses GFP::CED-11 in a *ced-11(n4666)* embryo [*ced-11(n4666); nEx2544[*$P_{egl\text{-}1}$*::gfp::ced-11*]. (*H–K*) Head of an L1 larva showing expression of *nIs790[*$P_{ced\text{-}11}$*::gfp::ced-11]; nEx2344[*$P_{evl\text{-}20}$*::mCherry::ph*. (*H*) DIC. (*I*) GFP::CED-11 expression in multiple cells. (*J*) Plasma membrane marker mCherry::PH. (*K*) Merged image shows colocalization of GFP::CED-11 and mCherry::PH.

double-mutant animals (Table 1). Thus, *ced-11* is required for the increase in refractility during apoptosis. We isolated six alleles of *ced-11* from the screen and later recovered a seventh allele, *n4666*, through a screen for *ced-11* deletion alleles (Fig. 1*E*). One mutant contained two mutations in *ced-11*, *n2745* and *n6046*. All *ced-11* alleles caused a reduction in the number of refractile apoptotic cells and a corresponding increase in the number of nonrefractile apoptotic cells (Fig. 1*F*).

To determine if CED-11 acts in the dying cell, we expressed a GFP::CED-11 translational fusion in *ced-11(n4666)* animals using an *egl-1* promoter and tested for rescue of the *ced-11* phenotype. EGL-1 is expressed in cells that undergo apoptosis (15). We found that 90% ($n = 72$) of $P_{egl\text{-}1}$*::gfp::ced-11*–expressing apoptotic cells were refractile, indicating that CED-11 functions in the dying cell to promote refractility (Fig. 1*G*). In addition, we occasionally observed engulfing cells that expressed $P_{egl\text{-}1}$*::gfp::ced-11* and contained nonrefractile GFP$^-$ apoptotic cells, showing that expression of CED-11 in the engulfing cell is not sufficient to rescue apoptotic cell refractility ($n = 4$). We conclude that CED-11 acts cell autonomously to increase refractility during apoptosis.

CED-11 Is a Presumptive TRP Channel and Can Localize to the Plasma Membrane. CED-11 shares sequence similarity with mammalian TRP family channels, sharing ~20% identity and 40% similarity with TRPM1 and TRPM3 (Fig. S1). TRP channels are nonselective cation channels, generally located in the plasma membrane and permeable to calcium and magnesium (16, 17). TRP channels have six membrane-spanning domains and a pore-forming region between transmembrane domains five and six.

We constructed a $P_{ced\text{-}11}$*::gfp::ced-11* translational reporter to determine the expression pattern of CED-11 (Fig. S2 *A–F*). $P_{ced\text{-}11}$*::gfp::ced-11* rescued the nonrefractile apoptotic cell phenotype of *ced-11(n4666)* mutant animals, indicating this fusion gene is functional and therefore likely expressed at sites required for function. GFP::CED-11 was expressed in both living and dying cells, as are other apoptotic cell-death proteins (18). We first detected GFP::CED-11 in pre–bean-stage embryos, in which it was expressed broadly and had a diffuse cytoplasmic localization (Fig. S2*B*). By the twofold embryonic stage, GFP::CED-11 had a more restricted pattern inside the cell and also could be seen on the plasma membrane (Fig. S2*D*). GFP::CED-11 was expressed in a few cells in the heads and tails of L1 larvae, where it was localized primarily to the plasma membrane (Fig. 1 *H–K*). We detected GFP::CED-11 in puncta at the perimeter of apoptotic cells (Fig. S2*G*).

***ced-11* Apoptotic Cells Have an Altered Ultrastructure.** To understand how changes in refractility correlate with other hallmarks of apoptosis, we examined the ultrastructure of apoptotic cells as visualized using EM in wild-type and *ced-11* mutant embryos. Previous EM studies of *C. elegans* revealed that after engulfment apoptotic cells progressively lose the integrity of their nuclei (19). Apoptotic cells with intact nuclei stain darkly compared with surrounding nonapoptotic cells and have a condensed cytoplasm and compact chromatin; we refer to such cells as "prebreakdown corpses." Apoptotic cells that do not have intact nuclei have cytoplasm that is lighter than surrounding nonapoptotic cells and contain small dark-staining fragments likely to be remnants of

Table 1. *ced-11* nonrefractile apoptotic cells are cells that normally undergo apoptosis

Genotype	No. refractile apoptotic cells	No. nonrefractile apoptotic cells
1.5-fold–stage embryos		
Wild-type	12.0 ± 1.8	0.0 ± 0.0
ced-11(n2744)	0.1 ± 0.3	4.8 ± 0.9
ced-3(n717)	0.0 ± 0.0	0.0 ± 0.0
ced-11(n2744); ced-3(n717)	0.0 ± 0.0	0.0 ± 0.0
*ced-4(n1162)**	0.0 ± 0.0	0.0 ± 0.0
*ced-4(n1162) ced-11(n2744)**	0.0 ± 0.0	0.0 ± 0.0
Threefold-stage embryos		
ced-5(n1812)	27.6 ± 3.1	1.1 ± 1.1
ced-11(n2744); ced-5(n1812)	1.0 ± 1.1	24.3 ± 4.3
ced-5(n1812) ced-3(n717)	0.3 ± 0.4	0.1 ± 0.3
ced-11(n2744); ced-5(n1812) ced-3(n717)	0.6 ± 0.8	0.5 ± 0.8

Apoptotic cells were identified by DIC. Data are shown as mean ± SD; $n > 20$.
*Strains contain *dpy-17(e164)*.

CELL BIOLOGY

membranes and chromatin; we refer to such cells as "postbreakdown corpses" (19, 20). Dark staining as visualized in EM is caused by the binding of electron-dense dyes to lipids and proteins, and it has been proposed that the increased electron density of prebreakdown apoptotic cells results from an increase in the concentration of macromolecules (21).

We considered cells that appeared to be engulfed to be apoptotic. As reported by Robertson and Thomas (19), in wild-type embryos prebreakdown apoptotic cells stained darker than living cells, with a shrunken cytoplasm, bloated organelles, and condensed chromatin (Fig. 2*A* and Fig. S3 *A* and *B*). By contrast, in *ced-11* embryos prebreakdown apoptotic cells did not stain darkly and generally looked similar to living cells, although they were still rounded and displayed some apoptotic cell features, including chromatin condensation and organelle bloating (Fig. 2 *B* and *C* and Fig. S3 *C–E*). We observed the absence of dark staining in the prebreakdown apoptotic cells of *ced-11* embryos in embryos of different ages, including before the bean-comma stage and after the 1.5-fold stage (Fig. S3 *A–D*). We conclude that *ced-11* is required for an increase in electron-dense staining during apoptosis.

Also, as reported by Robertson and Thomson (19), the postbreakdown corpses of wild-type embryos contained membranous whorls and remnants of chromatin, and the cytoplasm did not stain darkly (Fig. 2*D* and Fig. S4*A*). The postbreakdown corpses of *ced-11* animals looked similar to those of the wild type, indicating that apoptotic cells in *ced-11* animals reach late stages of degradation (Fig. 2 *E* and *F* and Fig. S4 *B* and *C*).

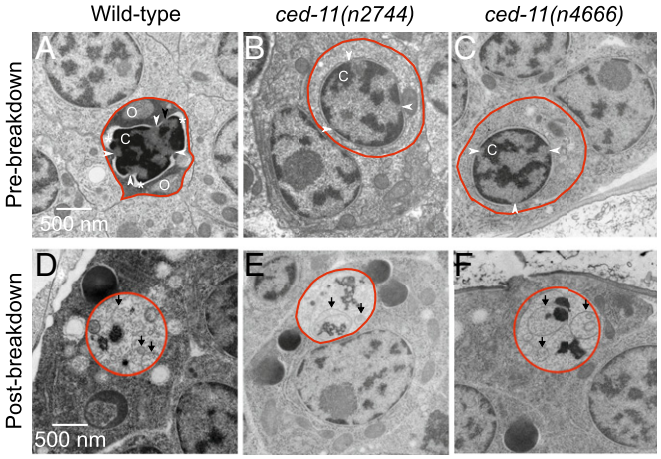

G	Wild-type	*ced-11 (n2744)*	*ced-11 (n4666)*
% wrinkled nuclei	40% (10/25)	0% (0/11)	0% (0/21)
% nuclear separation	60% (15/25)	9% (1/11)	19% (4/21)

Fig. 2. Apoptotic cells in *ced-11* animals have altered ultrastructure. (*A–F*) Electron micrographs of engulfed apoptotic cells (outlined in red). (*A*) A prebreakdown apoptotic cell in a wild-type embryo stained darkly and had a wrinkled nucleus and separation of the nuclear membrane (indicated by the asterisk). The arrowheads indicate the nuclear pore junction. C, condensed chromatin; O, bloated organelle. (*B* and *C*) Prebreakdown apoptotic cells in *ced-11(n2744)* (*B*) and *ced-11(n4666)* (*C*) embryos did not stain darkly and were not distinct from the surrounding living cells. (*D–F*) Apoptotic corpses postbreakdown in wild-type (*D*), *ced-11(n2744)* (*E*), and *ced-11(n4666)* (*F*) embryos contained membranous whorls and did not stain darkly. Arrows indicate a membranous whorl. (*G*) Percent of prebreakdown apoptotic cells in wild-type and *ced-11* embryos with wrinkled nuclei and nuclear separation.

In addition to the reduction in electron-dense staining, *ced-11* prebreakdown apoptotic cells appeared to differ in nuclear architecture. Prebreakdown apoptotic cells in wild-type embryos often had wrinkled nuclei (40%) and separation between the nucleus and cytoplasm (60%), although nuclear pore junctions could still be seen (Fig. 2*G*). Nuclear wrinkling and separation of the nucleus and cytoplasm might reflect altered structural integrity of the nuclear membrane. By contrast, prebreakdown apoptotic cells in *ced-11* embryos did not have wrinkled nuclei and showed nuclear–cytoplasm separation less frequently (about 15%) (Fig. 2*G*).

Engulfment Is Normal in *ced-11* Mutants. Next we asked if *ced-11* apoptotic cells could be recognized and engulfed normally. We used time-lapse videos of embryos expressing a $P_{ced\text{-}1}$*::ced-1::gfp* translational fusion to monitor the engulfment of three cells (C1, C2, and C3) that die during ventral enclosure of the embryo, when the epidermal sheets meet at the ventral midline (Fig. 3 *A–D*) (22). CED-1 is a transmembrane receptor that is expressed in engulfing cells and that clusters around apoptotic cells and mediates their engulfment (23). We observed that C1, C2, and C3 were engulfed during ventral enclosure in both wild-type and *ced-11* mutant embryos, indicating that both the onset of apoptosis and engulfment are grossly normal (Fig. 3 *A* and *B*). In addition, engulfment took a normal length of time in *ced-11* mutant embryos, ∼6 min, and CED-1::GFP was removed from the phagosomes at a normal rate, showing that both engulfment and the beginning of the phagosome maturation process are normal (Fig. 3*E*). We conclude that *ced-11* is required for the highly refractile morphology of apoptotic cells but is not required for the onset of apoptosis or for engulfment.

***ced-11* Apoptotic Cells Are Larger.** We noticed that apoptotic cells in *ced-11* embryos look larger than apoptotic cells in wild-type embryos. To quantify this difference, we measured the sizes of apoptotic cell-containing phagosomes at the time of engulfment, using the time-lapse movies of CED-1::GFP that we used to determine that engulfment is normal in *ced-11* mutants. Newly engulfed apoptotic cells in *ced-11* embryos were larger than apoptotic cells in wild-type embryos, with an average diameter of 2.7 μm vs. 2.3 μm (Fig. 4*A*). In addition, we measured the size of the apoptotic cells 2 min after engulfment and found that the wild-type apoptotic calls shrank by an average of 0.2 μm, whereas the *ced-11* apoptotic cells were unchanged in size (Fig. 4*B*). Thus, *ced-11* is required for apoptotic cell shrinkage. Apoptotic cells are generally spherical, so the 15% reduction in diameter at the time of engulfment corresponds to a 38% reduction in volume.

***ced-11* Apoptotic Cells Are Delayed in Degradation.** Because *ced-11* apoptotic cells have defects in cell shrinkage and look similar to living cells by EM, we tested whether apoptotic cells in *ced-11* embryos take longer to degrade. Engulfed apoptotic cells are degraded inside phagosomes. RAB-7 is recruited to apoptotic cell-containing phagosomes shortly after engulfment and persists on the phagosomes until cell-corpse degradation is complete (24). We used the disappearance of GFP::RAB-7 to assess cell-corpse degradation. We found that the cells in *ced-11* embryos took longer to degrade (60 min) than did wild-type apoptotic cells (45 min) (Fig. 4 *C* and *D*). In addition, we counted the number of GFP::RAB-7^{+} phagosomes in fourfold embryos and found the average number of such phagosomes was greater in the *ced-11* embryos (10 phagosomes) than in the wild type (five phagosomes), as is consistent with the delay in degradation (Fig. 4*E*). We conclude that *ced-11* promotes the degradation of apoptotic cells.

***ced-11* Mutants Do Not Have Extra Surviving Cells, but *ced-11* Mutation Can Enhance the Antiapoptotic Effects of Other Cell-Death Mutations.** Does CED-11 promote the deaths of apoptotic cells?

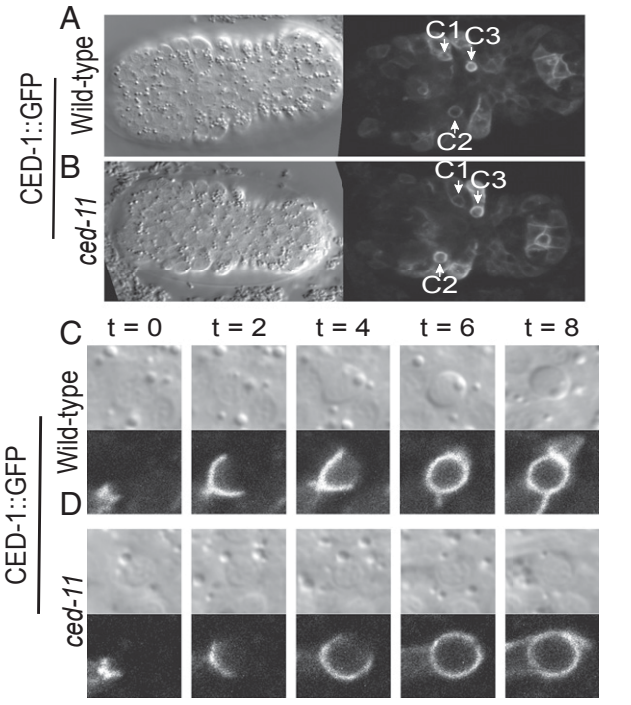

E Genotype	Engulfment	CED-1 removal
Wild-type	5.7 ± 1.9	5.6 ± 3.4
ced-11(n2744)	5.9 ± 1.7	5.6 ± 3.3
ced-11(n4666)	5.9 ± 1.7	5.7 ± 3.6

Fig. 3. Apoptotic cells in *ced-11* embryos are engulfed normally. (*A* and *B*) DIC (single focal plane, so not all corpses can be seen) and CED-1::GFP (merge of multiple focal planes) images of wild-type (*A*) and *ced-11* (*B*) embryos at the onset of ventral enclosure when apoptotic cells C1, C2, and C3 have been engulfed. All strains contain *enIs7* (P_{ced-1}::*ced-1*::*gfp*). (*C* and *D*) CED-1::GFP clustering around apoptotic cells as they are engulfed in wild-type (*C*) and *ced-11* (*D*) embryos with accompanying DIC images. Images were recorded every 2 min; time 0 is determined by the time of the image taken before CED-1::GFP began to encircle the apoptotic cell. Cells are engulfed at 6 min. (*E*) Average times for CED-1::GFP accumulation (engulfment) and removal (phagosome maturation) in wild-type and *ced-11* embryos. At least nine embryos and 26 apoptotic cells were analyzed for each genotype. Mean time is shown in minutes ± SD.

Using DIC, we noted that fewer apoptotic cells were observed in *ced-11* embryos than in the wild type (Table 1 and Fig. S5), suggesting that cell-death execution might be affected. We examined cell death in *ced-11* animals using two assays. First, we measured the survival of 16 pharyngeal cells that normally die during embryogenesis. Second, we measured the survival of five of seven cells (P2.aap and P9–12.aap) in the ventral nerve cord that normally die in late L1/early L2 larvae (25). We found no extra surviving cells in *ced-11* mutant animals with either assay (Fig. 5 *A* and *B* and Fig. S6). Because there was no extra cell survival in *ced-11* mutant animals, we propose that the apparent difference in apoptotic cell number results from the difficulty in distinguishing some *ced-11* nonrefractile apoptotic cells from living cells when using DIC.

We postulated that perhaps, even if *ced-11* promotes the deaths of apoptotic cells, if *ced-11* mutant cells are engulfed normally, they will not survive. *C. elegans* genes involved in engulfment have a weak effect on the cell-death killing process: In engulfment mutants, an average of 0.3–1.2 extra cells survive in the ventral nerve cord, as opposed to an average of 4.9 extra cells in mutants defective in the *ced-3* caspase gene (26). Therefore, we assayed cell death in double mutants defective in both *ced-11* and the engulfment process. We found that *ced-11* mutation enhances the ventral cord cell-death defect caused by mutations in the engulfment genes *ced-1*, *ced-2*, *ced-5*, *ced-6*, *ced-10*, and *ced-12*, nearly doubling the average number of surviving extra cells (Fig. 5*B* and Fig. S6). A *ced-11* mutation did not enhance the cell-death defect of *ced-7* mutants (Fig. 5*B*). *ced-7* is distinct from the other engulfment genes in other ways: *ced-7* is the only engulfment gene known to be required to act in the dying as well as in the engulfing cell, and *ced-7* mutants have a much stronger cell-death defect than the other engulfment mutants. We suggest that *ced-7* functions in the apoptotic cell to promote cell death, possibly in the same pathway as *ced-11*.

In addition, we analyzed the ability of *ced-11* mutations to enhance weak mutant alleles of the cell-death execution genes *ced-3* and *ced-4* and of a mutation in a gene that encodes a caspase target, *ced-8* (11, 15, 27). Mutation of *ced-11* enhanced cell survival caused by a mutation in the execution gene *ced-4* but

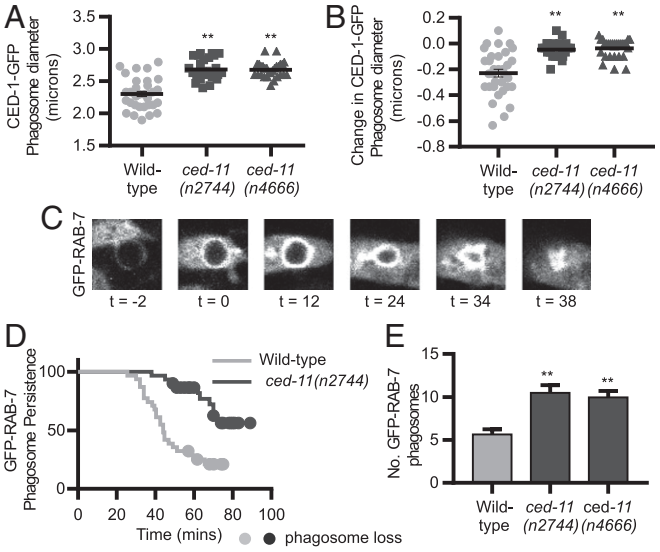

Fig. 4. *ced-11* is required for the decrease in cell volume and efficient degradation of apoptotic cells. (*A*) Diameter of apoptotic cells C1, C2, and C3 in wild-type, *ced-11(n2744)*, and *ced-11(n4666)* embryos at the time of CED-1::GFP engulfment. We measured the diameter at the most central Z section of each apoptotic cell using CED-1::GFP. Each dot, square, or triangle represents one apoptotic cell. Bars indicate the mean ± SD. At least nine embryos and 26 apoptotic cells were measured for each genotype. $^{**}P < 0.0001$, one-way ANOVA with Dennett's correction. (*B*) Change in the diameter of the apoptotic cells in *A*, between the time of engulfment and 2 min after engulfment. Each dot, square, or triangle represents one apoptotic cell. Bars indicate the mean ± SD. At least nine embryos and 26 apoptotic cells were measured for each genotype. $^{**}P < 0.0001$, one-way ANOVA with Dennett's correction. (*C*) Apoptotic cell degradation was measured using GRP::RAB-7. Time 0 is the onset of GFP::RAB-7 recruitment to the apoptotic cell containing the phagosome. The survival endpoint is when the GFP::RAB-7 apoptotic cell has shrunk and disappeared. (*D*) Kaplan–Meier survival curve of apoptotic cells (C1, C2, and C3) in wild-type and *ced-11(n2744)* embryos; GFP-RAB-7 was used to measure degradation times. Apoptotic cells were occasionally lost from the field of view around 50 min, when embryos started moving; circles indicate apoptotic cells that were lost to view before degradation was complete. Ten embryos and 30 apoptotic cells were evaluated for each genotype. $P < 0.0001$, Gehan–Breslow–Wilcoxon test. (*E*) Number of GFP::RAB-7^{+} phagosome-engulfed apoptotic cells in fourfold-stage embryos of the indicated genotypes. Bars indicate mean and SEM; $n > 50$. $^{**}P < 0.0001$, one-way ANOVA with Dennett's correction.

CELL BIOLOGY

A

Extra Cells in the Anterior Pharynx		
Genotype	No. extra cells	Range extra cells
Wild-type	0.04 ± 0.03	0-1
ced-3(n717)	13.2 ± 1.9	10-16
ced-11(n2744)	0.09 ± 0.06	0-1
ced-11(n4666)	0.0 ± 0.0	0

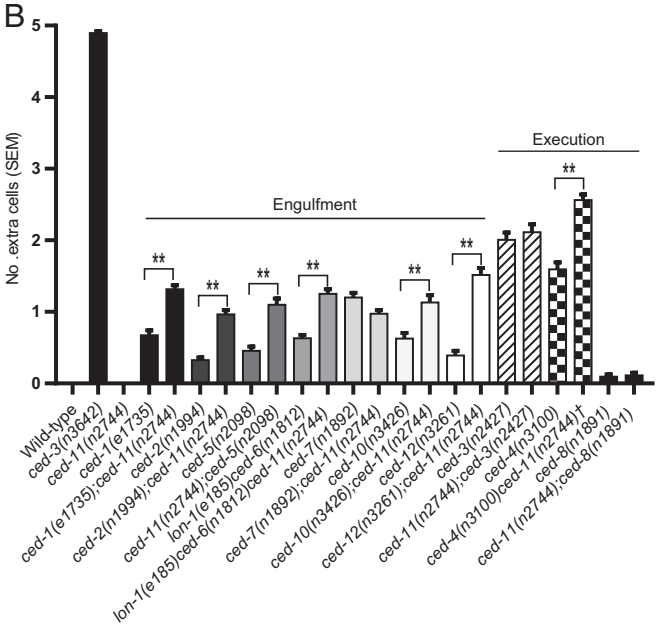

Fig. 5. Mutation of *ced-11* does not cause cell survival on its own but can enhance cell survival in other cell-death mutants. (*A*) Average number of extra cells present in the anterior pharynges of L3–L4 hermaphrodites. Data are shown as mean ± SD; $n > 20$). (*B*) Average number of extra cells in the ventral cords of L4 hermaphrodites. Error bars indicate SEM; $n > 100$. All strains contain *nIs106*. The *ced-11* allele used was *ced-11(n2744)*. The dagger indicates the presence of *dpy-18*. $^{**}P < 0.001$, one-way ANOVA with Sidak's multiple comparisons test.

did not enhance alleles of *ced-3* or *ced-8* (Fig. 5*B* and Fig. S6). *ced-4* has a proapoptotic isoform, *ced-4S*, which acts in the execution pathway with *ced-3*, and an antiapoptotic isoform, *ced-4L*, the function of which is less well understood. Perhaps *ced-4L* acts in parallel to *ced-11* to regulate cell death and *ced-4S*, *ced-3*, and *ced-8* act in the same pathway as *ced-11*. In any case, these data indicate that *ced-11* can facilitate cell killing.

Discussion

ced-11 is required for many but not all of the cellular changes that occur during apoptosis: shrinkage, increased refractility, increased electron density, and nuclear membrane wrinkling and separation, but not chromatin condensation, plasma membrane rounding, or engulfment. *ced-11* encodes a presumptive TRP channel based on sequence similarity to known TRP channels (17). Like most TRP channels, the CED-11 protein can localize to the plasma membrane as well as to internal membranes (16). *ced-11* acts downstream of *ced-3*, because *ced-3* is required for the initiation of cell death and *ced-11* is required for a subset of *ced-3*–dependent changes that contribute to cell death. That *ced-11* mutation does not enhance the cell-death defect of weak *ced-3* mutation strongly suggests that *ced-11* and *ced-3* act in the same pathway rather than in parallel to promote cell death. That *ced-11* mutation enhances cell survival in engulfment-mutant strains and results in defects in apoptotic cell degradation suggests that cellular changes driven by *ced-11* contribute to the process of cell death and cell degradation. Taken together, our data show that *ced-11* acts downstream of *ced-3* and in parallel to phagosome maturation to promote the death and degradation of the apoptotic cell (Fig. 6*A*). We propose that the delay in degradation in *ced-11* animals is caused by the defect in cell-volume reduction and that this degradation defect can be bypassed by the phagocytic pathway, although more slowly. If the dying cell is not engulfed and degraded by a phagosome, it has a greater chance of survival.

ced-11 is required for the reduction of cell volume during apoptosis. As noted above, cell shrinkage during apoptosis has been called "apoptotic volume decrease" (AVD) to differentiate it from RVD induced by osmotic challenge (8). AVD occurs in normotonic cellular conditions and has been proposed to be induced by the opening of potassium and chloride channels in the plasma membrane, causing an efflux of potassium and chloride ions followed by water (28–30). The mechanism for activating such channels during apoptosis is unknown. Multiple TRP channels have been implicated in cell-volume regulation (9, 31, 32). TRPV4 mediates a Ca^{2+} influx in response to hypoosmotic stress and had been hypothesized to stimulate calcium-activated potassium and chloride channels, resulting in RVD (32, 33). We propose that CED-11 contributes to AVD by a similar mechanism.

Apoptotic cells in *ced-11* animals fail to increase in refractility. The highly refractile appearance of apoptotic cells in *C. elegans* is the defining morphological feature used to differentiate living cells from dying cells, but the biological cause of the refractility is unknown. Refractility is known to increase with increased concentrations of proteins and other macromolecules but shows little or no change in response to changes in salt concentration, changes in pH, denaturation of proteins, or digestion of proteins to amino acids (34). The refractility of mammalian cells also increases during apoptosis, and it has been suggested that this increase reflects a decrease in intracellular water and a corresponding increase in the concentration of proteins and other macromolecules in the cell (35). The increased refractility of apoptotic cells observed in *C. elegans* could also result from an increase in the concentration of macromolecules. This hypothesis is supported by our observation that apoptotic cells in *ced-11* embryos do not stain darkly in EM. Electron-dense staining in EM reflects high concentrations of proteins and lipids (7). Furthermore, EM studies of mammalian cells in a hyperosmotic solution that induced cell shrinkage showed an increased electron density compared with cells in an iso-osmotic solution (36).

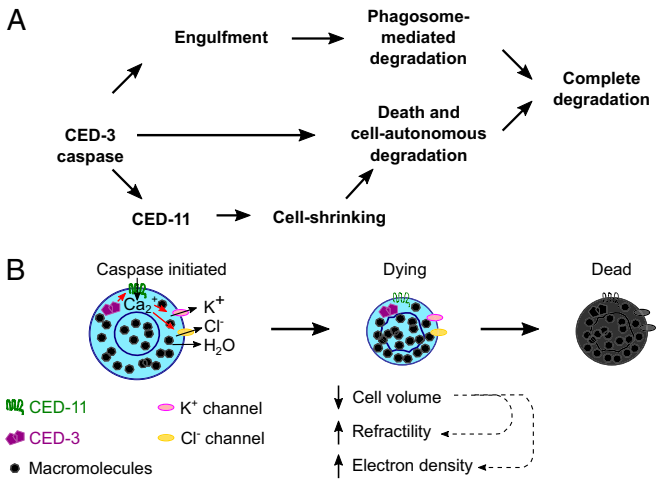

Fig. 6. Model for CED-11 function in apoptosis. CED-11 acts downstream of CED-3 to promote cell-autonomous death and degradation in parallel with engulfment and phagosome-mediated degradation. CED-11 is directly or indirectly activated by the CED-3 caspase. CED-11 activation results in a decrease in cell volume, driving an increase in macromolecule density and leading to the observed increases in cellular refractility and electron density. CED-11–mediated changes in the apoptotic cell promote its death and degradation. (*A*) Pathway. (*B*) Schematic.

We propose that CED-11 functions as a TRP channel to alter ion flow and promote a cell volume decrease through a loss of intracellular water that causes an increased concentration of proteins and other macromolecules, resulting in the observed increase in cellular refractility and electron density (Fig. 6*B*). More specifically, we hypothesize that activation of CED-11 in apoptotic cells causes an influx of Ca^{2+}, which activates Ca^{2+}-activated K^+ and Cl^- channels in the cell and leads to an efflux of K^+ down the concentration gradient and an efflux of Cl^- to maintain electroneutrality, followed by an efflux of water down the osmotic gradient. Consequently, cell volume is reduced, and an increase in the concentration of macromolecules in the cell results in the increase in refractility and electron density. The reduction of cell volume might also contribute to the observed changes in nuclear membrane structure. In conclusion, we find that a presumptive TRP channel acts downstream of caspase activation to promote cell shrinkage and contributes to apoptotic cell degradation in parallel to the phagosome degradation pathway.

Materials and Methods

A more complete description is available in *SI Materials and Methods*.

***C. elegans* Strains.** *C. elegans* strains were cultured at 20 °C as described previously (37) and are listed in *SI Materials and Methods*.

Cell-Death Assays. The anterior pharynx (26) and ventral cord (25) cell-death assays were performed as described. One-way ANOVA with Sidak's multiple comparisons test and Student's *t* test were performed using GraphPad Prism.

Assays for Engulfment, Degradation, and Cell Diameter. The engulfment and degradation assays were performed as described (24). We measured the diameter at the most central Z section of each apoptotic cell at the moment of engulfment. For each cell the diameter was measured three times at equidistant cross-sections, and these values were averaged.

ACKNOWLEDGMENTS. We thank H. Johnsen, A. Corrionero Saiz, and C. Engert for comments about this manuscript; V. Dwivedi for discussions and plasmid cloning; and Z. Zhou for strains and plasmids. Some strains were provided by the *Caenorhabditis* Genetics Center, which is funded by the NIH Office of Research Infrastructure Programs (P40 OD010440). This work was supported by the Howard Hughes Medical Institute. K.D. was supported in part by NIH Pre-Doctoral Training Grant T32GM007287. H.R.H. is the David H. Koch Professor of Biology at the Massachusetts Institute of Technology and is an Investigator of the Howard Hughes Medical Institute.

1. Kerr JFR, Wyllie AH, Currie AR (1972) Apoptosis: A basic biological phenomenon with wide-ranging implications in tissue kinetics. *Br J Cancer* 26:239–257.
2. Wyllie AH (1980) Glucocorticoid-induced thymocyte apoptosis is associated with endogenous endonuclease activation. *Nature* 284:555–556.
3. Igney FH, Krammer PH (2002) Death and anti-death: Tumour resistance to apoptosis. *Nat Rev Cancer* 2:277–288.
4. Poon IKH, Lucas CD, Rossi AG, Ravichandran KS (2014) Apoptotic cell clearance: Basic biology and therapeutic potential. *Nat Rev Immunol* 14:166–180.
5. Lüthi AU, Martin SJ (2007) The CASBAH: A searchable database of caspase substrates. *Cell Death Differ* 14:641–650.
6. Yuan J, Shaham S, Ledoux S, Ellis HM, Horvitz HR (1993) The *C. elegans* cell death gene *ced-3* encodes a protein similar to mammalian interleukin-1 β-converting enzyme. *Cell* 75:641–652.
7. Kerr JFR (1971) Shrinkage necrosis: A distinct mode of cellular death. *J Pathol* 105: 13–20.
8. Maeno E, Ishizaki Y, Kanaseki T, Hazama A, Okada Y (2000) Normotonic cell shrinkage because of disordered volume regulation is an early prerequisite to apoptosis. *Proc Natl Acad Sci USA* 97:9487–9492.
9. Jentsch TJ (2016) VRACs and other ion channels and transporters in the regulation of cell volume and beyond. *Nat Rev Mol Cell Biol* 17:293–307.
10. Sulston JE, Horvitz HR (1977) Post-embryonic cell lineages of the nematode, *Caenorhabditis elegans*. *Dev Biol* 56:110–156.
11. Ellis HM, Horvitz HR (1986) Genetic control of programmed cell death in the nematode *C. elegans*. *Cell* 44:817–829.
12. Hedgecock EM, Sulston JE, Thomson JN (1983) Mutations affecting programmed cell deaths in the nematode *Caenorhabditis elegans*. *Science* 220:1277–1279.
13. Jin M, Berrout J, O'Neil RG (2011) Regulation of TRP channels by osmomechanical stress. *TRP Channels*, ed Zhu MX (CRC /Taylor & Francis, Boca Raton, FL).
14. Clapham DE (2003) TRP channels as cellular sensors. *Nature* 426:517–524.
15. Conradt B, Horvitz HR (1998) The *C. elegans* protein EGL-1 is required for programmed cell death and interacts with the Bcl-2-like protein CED-9. *Cell* 93:519–529.
16. Montell C, Birnbaumer L, Flockerzi V (2002) The TRP channels, a remarkably functional family. *Cell* 108:595–598.
17. Harteneck C, Plant TD, Schultz G (2000) From worm to man: Three subfamilies of TRP channels. *Trends Neurosci* 23:159–166.
18. Chen F, et al. (2000) Translocation of *C. elegans* CED-4 to nuclear membranes during programmed cell death. *Science* 287:1485–1489.
19. Robertson AMG, Thomson JN (1982) Morphology of programmed cell death in the ventral nerve cord of *Caenorhabditis elegans* larvae. *J Embryol Exp Morphol* 67: 89–100.
20. Sulston JE, Schierenberg E, White JG, Thomson JN (1983) The embryonic cell lineage of the nematode *Caenorhabditis elegans*. *Dev Biol* 100:64–119.
21. Klion FM, Schaffner F (1966) The ultrastructure of acidophilic "Councilman-like" bodies in the liver. *Am J Pathol* 48:755–767.
22. Yu X, Lu N, Zhou Z (2008) Phagocytic receptor CED-1 initiates a signaling pathway for degrading engulfed apoptotic cells. *PLoS Biol* 6:e61.
23. Zhou Z, Hartwieg E, Horvitz HR (2001) CED-1 is a transmembrane receptor that mediates cell corpse engulfment in *C. elegans*. *Cell* 104:43–56.
24. Li Z, Lu N, He X, Zhou Z (2013) Monitoring the clearance of apoptotic and necrotic cells in the nematode *Caenorhabditis elegans*. *Methods Mol Biol* 1004:183–202.
25. Schwartz HT (2007) A protocol describing pharynx counts and a review of other assays of apoptotic cell death in the nematode worm *Caenorhabditis elegans*. *Nat Protoc* 2: 705–714.
26. Reddien PW, Cameron S, Horvitz HR (2001) Phagocytosis promotes programmed cell death in *C. elegans*. *Nature* 412:198–202.
27. Stanfield GM, Horvitz HR (2000) The *ced-8* gene controls the timing of programmed cell deaths in *C. elegans*. *Mol Cell* 5:423–433.
28. Barbiero G, Duranti F, Bonelli G, Amenta JS, Baccino FM (1995) Intracellular ionic variations in the apoptotic death of L cells by inhibitors of cell cycle progression. *Exp Cell Res* 217:410–418.
29. Beauvais F, Michel L, Dubertret L (1995) Human eosinophils in culture undergo a striking and rapid shrinkage during apoptosis. Role of K+ channels. *J Leukoc Biol* 57: 851–855.
30. Dezaki K, Maeno E, Sato K, Akita T, Okada Y (2012) Early-phase occurrence of K+ and Cl- efflux in addition to Ca 2+ mobilization is a prerequisite to apoptosis in HeLa cells. *Apoptosis* 17:821–831.
31. Numata T, Shimizu T, Okada Y (2007) TRPM7 is a stretch- and swelling-activated cation channel involved in volume regulation in human epithelial cells. *Am J Physiol Cell Physiol* 292:C460–C467.
32. Pan Z, et al. (2008) Dependence of regulatory volume decrease on transient receptor potential vanilloid 4 (TRPV4) expression in human corneal epithelial cells. *Cell Calcium* 44:374–385.
33. Becker D, Blase C, Bereiter-Hahn J, Jendrach M (2005) TRPV4 exhibits a functional role in cell-volume regulation. *J Cell Sci* 118:2435–2440.
34. Barer R, Joseph S (1954) Refractometry of living cells. *J Cell Sci* 95:399–423.
35. Model MA, Schonbrun E (2013) Optical determination of intracellular water in apoptotic cells. *J Physiol* 591:5843–5849.
36. Delpire E, Duchêne C, Goessens G, Gilles R (1985) Effects of osmotic shocks on the ultrastructure of different tissues and cell types. *Exp Cell Res* 160:106–116.
37. Brenner S (1974) The genetics of *Caenorhabditis elegans*. *Genetics* 77:71–94.
38. Ma H, Kunes S, Schatz PJ, Botstein D (1987) Plasmid construction by homologous recombination in yeast. *Gene* 58:201–216.
39. Hirose T, Galvin BD, Horvitz HR (2010) Six and Eya promote apoptosis through direct transcriptional activation of the proapoptotic BH3-only gene *egl-1* in *Caenorhabditis elegans*. *Proc Natl Acad Sci USA* 107:15479–15484.